American Society of Hematology
2021 L Street NW, Suite 900,
Washington, DC 20036
Phone: 202-776-0544 | Fax 202-776-0545
editorial@hematology.org

Disulfide Exchange in von Willebrand factor Dimerization in the Golgi

Tracking no: BLD-2020-005989R1

Xianchi Dong (Nanjing University, China) Timothy Springer (Boston Children's Hospital/Harvard Medical School, United States)

Abstract:

Conflict of interest: No COI declared

COI notes:

Preprint server: No;

Author contributions and disclosures: T.A.S and X.D. each contributed to conception, experimental design, and writing the manuscript.

Non-author contributions and disclosures: No;

Agreement to Share Publication-Related Data and Data Sharing Statement: For original data, please contact springer@crystal.harvard.edu

Clinical trial registration information (if any):

Disulfide Exchange in Multimerization of von Willebrand factor and Gel-forming Mucins

Short Title: Disulfide Exchange in D3 Assembly Dimerization

Xianchi Dong[1] and Timothy A. Springer[# 2]

[1]State Key Laboratory of Pharmaceutical Biotechnology, School of Life Sciences, Nanjing University, Nanjing, China

[2] Department of Biological Chemistry and Molecular Pharmacology and Department of Pediatrics, Harvard Medical School; Program in Cellular and Molecular Medicine, Boston Children's Hospital, 3 Blackfan Circle, Boston, MA 02115, USA

[#] To whom correspondence should be addressed: springer@crystal.harvard.edu; 617-713-8200

Von Willebrand factor (VWF) monomers dimerize through their C-terminal domain in the endoplasmic reticulum (ER). The unusual process of disulfide bond formation between N-terminal D'D3 assemblies (Fig. 1) of neighboring dimers during tubule formation in the Golgi then forms the ultralong, tail-to-tail, head-to-head concatemers required for VWF activation in hemostasis[1-5]. C-terminally-truncated VWF fragments are secreted as mixtures of monomers and dimers; the monomers contain two free cysteines, Cys-1099 and Cys-1142, which were proposed to form the dimerizing inter-chain disulfide bonds[6]. However, chemical determination of disulfide bonds in VWF is challenging[7-9] and only the Cys-1142/Cys-1142' disulfide has been confirmed[1]. Surprisingly, a recent VWF D'D3 monomer crystal structure showed burial of Cys-1099 and Cys-1142, thus revealing how these residues are protected from disulfide bond formation in the ER, but little about disulfide bond formation in the Golgi[9]. Gel-forming mucins contain D assemblies homologous to those of VWF and also form multimers in the Golgi[10]; however, in mucin MUC2, homologues of VWF Cys-1142 and Cys-1097 but not Cys-1099 formed dimerizing disulfides. Multiple explanations for the discrepancy were proposed but not resolved[11]. Here, we present evidence suggesting that disulfide exchange between three Cys residues in VWF frees Cys-1097 to form a dimerizing disulfide bond.

In the monomeric D'D3 crystal structure, Cys-1099 and Cys-1142 were mutated to alanine and modeled as Cys. Cys-1099, with disulfide-bonded Cys-1091 and Cys-1097, forms a triad of three Cys residues that locate close to one another in the C8-3 module (Figs. 1C and 2). The free sulfhydryl group of Cys-1099 is shielded by the VWD3 module, making Cys-1099 inaccessible for disulfide bond formation[9]. Furthermore, movement of Cys-1099 is limited by its position in an α-helix with two disulfide bonds to other structural elements in C8-3.

In contrast, rearrangement of disulfide bonds within the cysteine triad is highly feasible, a possibility we were careful not to exclude with the previous conclusion "that structural rearrangements are required for D3 dimerization in the Golgi"[9]. The Cys-1099 SH group is only 4.7 Å away from the disulfide-bonded sulfur atoms of Cys-1091 and Cys-1097, with no nearby atoms to hinder nucleophilic attack by Cys-1099 on the disulfide. Furthermore, the Cys-1091/Cys-1097 disulfide is exposed to solvent in a loop that contains a Gly residue that can confer flexibility and is invariant in VWF and mucins (Fig. 2C). Thus, the most plausible mechanism for exposure of cysteine for dimerization is nucleophilic attack by the S^- anion of C1099 on the disulfide, thereby freeing Cys-1097 for formation of a disulfide bond to another monomer. Given the high local concentrations of these residues within the triad loop, disulfide exchange among them is likely to be in rapid equilibrium. At neutral pH, the equilibrium favors free Cys-1099[6]. At acidic pH, interactions among D assemblies at the ends of growing VWF tubules in the Golgi may favor free Cys-1097, the homologue of which in MUC2 forms the interchain disulfide[11]. The triad loop also contains Glu-1092 and Asp-1096, which are always acidic or invariant, respectively, in VWF and gel-forming mucins (Fig. 2C). These acidic residues might have a dual function in deprotonating the Cys SH group for nucleophilic attack and ionically repelling interactions between triad loops in different monomers in the ER to prevent premature D3 dimerization.

To test the feasibility of VWF dimerization through Cys-1097, we built a dimer model. The VWF D3 assembly aligns well by sequence with mucins (38% identity with MUC2) with no sequence insertions or deletions in the key C8-3 module among VWF and all five, human, gel-forming mucins (Fig. 1C and D and Supplemental Fig. 1). Monomeric VWF D'D3[9] was superimposed on each monomer of dimeric MUC2 D3[11] with an RMSD of 1.3 Å over 330 residues per monomer. Using this dimeric template and homology modeling, we constructed a robust model of dimeric VWF D'D3 (Fig. 1E-G, Fig. 2B, and supplemental Fig. 1).

The feasibility of the model is supported by the structure of the dimeric interface. The only significant structural differences between the monomer and dimer in this interface are in C8-3 module residues 1090-1099, which comprise the loop containing the cysteine triad, and in TIL3 module residues 1131-1143, which contain Cys-1142 (black overlines in Fig. 1C-D; Fig. 2A-C). In between, residues

1122-1130 are in the interface but are in identical backbone conformations in dimeric MUC2 and monomeric VWF. Preservation of the geometry in monomeric VWF at dimer interfacial residues 1122-1130 with the ability to properly model interfacial disulfide formation in the dimer support our model of disulfide exchange to free Cys-1097 prior to 1097-1097' disulfide formation.

The model suggests that D3 dimerization is accompanied by no change in backbone position of Cys-1099, which is well embedded in an α-helix. Only the sidechain of Cys-1099 rotates to form a disulfide to Cys-1091, which moves in its loop. Residues 1096-1098 in the cysteine triad loop alter to α-helical conformation and add on to the end of the α4-helix bearing Cys-1099 (Fig. 2C). In its new helical conformation, Cys-1097 disulfide bonds across the dimer interface to its mate in the other monomer. Furthermore, Asp-1096 in each monomer forms hydrogen bonds to backbone across the dimer interface (Fig. 2A-C). To make the turn between the α4-helix and the loop bearing Cys-1091, Gly-1095 changes to the Lα conformation, which is only allowed for glycine, explaining the invariance of this residue in VWF and gel-forming mucins. Dimerization further requires the loop that buries Cys-1142 in VWF monomers to partially unfurl with an 11 Å movement of Cys-1142 to disulfide bond across the dimer interface.

In the loop bearing the cysteine triad, the three cysteines, Gly-1095, and Asp-1096 and their equivalents are invariant in all sequenced animal species in VWF, MUC2, MUC5AC, MUC5B, and MUC6. Our results thus suggest that not only VWF, but also four of the five gel-forming mucins, have a free, buried Cys-1099 equivalent that is protected from disulfide formation in the ER and that undergoes disulfide exchange in the Golgi so that the more exposed Cys-1097 equivalent is free to form the dimerizing disulfide bond. In contrast, Muc19 contains only the Cys-1091 equivalent (Fig. 2C), has Lys in place of VWF Asp-1096, and thus has a different conformation at the dimerization interface which might involve dimerization through the equivalent of Cys-1091. We welcome confirmation of our model by determining whether single or double mutations in the cysteine triad in VWF or mucins compromise normal multimerization in the Golgi or lead to aberrant multimerization such as by exposing Cys-1097 or its equivalent in mucins in the ER.

As originally proposed by Sadler[1] and found in MUC2 dimers[11], monomers align parallel to one another in D'D3 dimers, with the two-fold rotational symmetry (dyad) axis passing between the Cys-1097/Cys-1097' and Cys-1142/Cys-1142' pairs (Fig. 1E-G). EM class averages of dimers containing D'D3 linked to A1 through the flexible mucin segment[12] cross-correlate well to the model, show horn-like D' projections and A1 domain positions not far from the C-terminus of D3, and provide further confirmation for the proposed dimerization mode (Fig. 1H).

What triggers D3 dimerization? In the trans-Golgi, the D1D2 prodomain packs against D'D3 and these D1-D3 units in turn pack further with one another and assemble into tubules with helical symmetry that characterize Weibel-Palade bodies[3-5]. D1D2 is required for both tubule assembly[3] and D3-D3 dimer formation[13Wise, 1988,14,15]. D1D2 was proposed to be an oxidoreductase with cysteine residues in a CGLC sequence that functioned, as in protein disulfide isomerases, to catalyze oxidation of the dimerizing disulfides in D3 [16]. D3 is highly homologous to D1 and D2 and has the same CGLC sequence[5]. The D3 structure shows that the CGLC sequence is highly buried in the VWD module and that its cysteines disulfide link to other VWD cysteines distal in sequence and could not be alternately reduced and disulfide linked to one another as required in an oxidoreductase[9]. Disruption of VWF multimer formation when an extra glycine is inserted into D1 or D2 CGLC sequences [16] therefore should be reinterpreted as a disruption of domain conformation that might alter packing in tubules.

This reinterpretation supports Sadler's model that tubule formation in the trans-Golgi facilitates VWF N-terminal dimerization by juxtaposing D3 domains[3]. Between the ER and the trans-Golgi, the pH decreases from 7.2 to 5.8 and a pH of ~5.8 is required for both VWF tubule formation *in vitro* and multimerization in vivo and in vitro[3,15,17]. Histidine has a pK of ~6. Mutation of His residues that are

conserved in VWF and mucins has shown that histidines in D2 and D1 regulate VWF multimerization[10]; furthermore, homology to D3 shows that these His residues are distributed around the periphery of the D1 and D2 assemblies, where contacts between neighboring D assemblies in tubules are expected to occur[3,5]. Therefore, we propose that the pH-dependent contacts between D assemblies as they assemble on the growing ends of tubules in the trans-Golgi, including between juxtaposed D3 assemblies, trigger conformational changes that stabilize D3 dimer formation. These changes would stabilize disulfide exchange in the cysteine triad loop freeing Cys-1097 and a new conformation of this loop, a new conformation of the loop containing Cys-1142, and close juxtaposition of these residues with their mates in the neighboring D3 assembly.

How are the Cys-1097/Cys-1097' and Cys-1142/Cys-1142' disulfides oxidized? As we propose that disulfide exchange in the cysteine triad loop occurs directly, the redox function of a protein disulfide isomerase is not required; its oxidase function would suffice. Alternatively, a sulfhydryl oxidase, such as QSOX1, which localizes to the Golgi, might catalyze disulfide formation[18].

Figure Legends

Figure 1. Modeling D`D3 dimerization. A. Domain architecture and position of dimerizing cysteine residues (red vertical lines with S) in D'D3 assembly (upper) and VWF monomer (lower). Modified from Springer[5]. B. Solvent accessible surface of D'D3[9]. C and D. Sequence alignments of D3 C8-3 and TIL3 modules in VWF and gel-forming mucins (see Supplementary Figure 1 for VWD3 and E3). Cysteines implicated in disulfide exchange and inter-chain disulfides are asterisked and highlighted in red while those that form intra-chain disulfides are linked and highlighted in other colors. E-G. The D'D3 dimer model is shown as a solvent accessible surface colored by module with its 2-fold rotational axis as a double-ended arrow colored green on one end and blue on the other. D3 C-termini in E3 are marked with large light blue spheres. Residues mutated in VWF disease that cause loss of VWF binding (type 2M) and no other phenotypes (types 1, 3, 2A, and 2B) are marked with large red spheres. VWF tubules in Weibel-Palade bodies also have a dyad symmetry axis[3,4] to which the D'D3 dimer axis must be parallel. VWF biology suggests that the dimer axis end colored green in Fig. 1E-G would orient toward the outside rather than the inside of tubules. This side links to A1 and the VWF C-terminus and bears VWF disease mutations that specifically abolish Factor VIII binding[9], which occurs during biosynthesis[19]. A model of VWF tubules based on MUC2 filaments also supports this orientation[20]. The dimer model was created with Modeller 9.6[21] as described in the text with each monomer templated with the segments of VWF and MUC2 (PDB ID 6N29 and 6RBF, respectively) shown in Supplemental Fig. S2. H. Cross-correlation of the D`D3 dimer model to three EM class averages of D'D3-A1 dimers[12] was as described[12,22]. The best-correlating D'D3 dimer orientation is shown enlarged as a ribbon diagram with coloring similar to that in E-G and with spheres at C-termini of E3 to show where the mucin linker to A1 attaches. Owing to flexibility of this linker, A1 (a round globule) appears in different orientations or does not appear in class averages.

Figure 2. Conformational change in VWF C8-3 and TIL3 during dimerization. A and B. Comparison of monomeric crystal structure model (A) and dimeric homology model (B) of D3. The monomer on the left is color-coded identically in A and B. Each module is labeled and has a distinct color for carbon atoms, except regions that change substantially in conformation upon dimerization are colored magenta. The other monomer on the right in the dimer in (B) lacks the color code for conformational change and its modules are shown in slightly different colors than in A. Its module and sidechain names are distinguished with an appended apostrophe. Sidechains of cysteines and other selected residues are shown as sticks with yellow sulfurs and red oxygens. Additionally, sulfur atoms of cysteines in the triad in C8-3 and C1142 in TIL3 are shown as spheres. Dashed black arrows represent vectors for change in position of the sulfur atoms. Backbone Cα atoms of Cys triad residues are connected with cyan lines in A. The hydrogen bonds between the Asp-1096 sidechain and mainchain of the other monomer in the dimer are shown as red dashed lines for one of two reciprocal interactions in B. C. Sequence alignment of the cysteine triad in human VWF and gel-like mucins. In VWF and MUC2, cysteines in intra-chain disulfides are green and those as free cysteines in the VWF monomer or in inter-chain linkages in dimers are red. Cysteines in other mucins are black; however, four have cysteine triad sequences highly identical among VWF and four mucins and are predicted to undergo disulfide exchange between monomers and dimers, like VWF. MUC19 differs substantially in the same region, including having only one cysteine. It is predicted to be free in the monomer and disulfide linked in the dimer, much like Cys-1142 in VWF and its equivalent in all gel-like mucins.

Acknowledgements
Supported by NIH grant R01-HL148755 from NHLBI.

Authorship
T.A.S and X.D. each contributed to conception, experimental design, and writing the manuscript.

Conflict-of-interest Statements
The authors declare no competing financial interests.

Data sharing

For original data, please email the corresponding author.

References

1. Dong Z, Thoma RS, Crimmins DL, McCourt DW, Tuley EA, Sadler JE. Disulfide bonds required to assemble functional von Willebrand factor multimers. *J Biol Chem*. 1994;269(9):6753-6758.

2. Sadler JE. Biochemistry and genetics of von Willebrand factor. *Annu Rev Biochem*. 1998;67:395-424.

3. Huang RH, Wang Y, Roth R, et al. Assembly of Weibel-Palade body-like tubules from N-terminal domains of von Willebrand factor. *Proc Natl Acad Sci U S A*. 2008;105(2):482-487.

4. Berriman JA, Li S, Hewlett LJ, et al. Structural organization of Weibel-Palade bodies revealed by cryo-EM of vitrified endothelial cells. *Proc Natl Acad Sci U S A*. 2009;106(41):17407-17412.

5. Springer T. von Willebrand factor, Jedi knight of the bloodstream. *Blood*. 2014;124(9):1412-1425.

6. Purvis AR, Gross J, Dang LT, et al. Two Cys residues essential for von Willebrand factor multimer assembly in the Golgi. *Proc Natl Acad Sci U S A*. 2007;104(40):15647-15652.

7. Marti T, Rosselet SJ, Titani K, Walsh KA. Identification of disulfide-bridged substructures within human von Willebrand factor. *Biochemistry*. 1987;26(25):8099-8109.

8. Zhou YF, Eng E, Zhu J, Lu C, Walz T, Springer TA. Sequence and structure relationships within von Willebrand factor. *Blood*. 2012;120(2):449-458.

9. Dong X, Leksa NC, Chhabra ES, et al. The von Willebrand factor D'D3 assembly and structural principles for factor VIII binding and concatemer biogenesis. *Blood*. 2019;133(14):1523-1533.

10. Dang LT, Purvis AR, Huang RH, Westfield LA, Sadler JE. Phylogenetic and functional analysis of histidine residues essential for pH-dependent multimerization of von Willebrand factor. *J Biol Chem*. 2011;286:25763-25769.

11. Javitt G, Calvo MLG, Albert L, et al. Intestinal Gel-Forming Mucins Polymerize by Disulfide-Mediated Dimerization of D3 Domains. *J Mol Biol*. 2019.

12. Zhou Y, Eng E, Nishida N, Lu C, Walz T, Springer TA. A pH-regulated dimeric bouquet in the structure of von Willebrand factor. *EMBO J*. 2011;30(19):4098-4111.

13. Verweij CL, Hart M, Pannekoek H. Expression of variant von Willebrand factor (vWF) cDNA in heterologous cells: requirement of the pro-polypeptide in vWF multimer formation. *EMBO J*. 1987;6(10):2885-2890.

14. Wise RJ, Pittman DD, Handin RI, Kaufman RJ, Orkin SH. The propeptide of von Willebrand factor independently mediates the assembly of von Willebrand multimers. *Cell*. 1988;52(2):229-236.

15. Mayadas TN, Wagner DD. In vitro multimerization of von Willebrand factor is triggered by low pH. Importance of the propolypeptide and free sulfhydryls. *J Biol Chem*. 1989;264(23):13497-13503.

16. Mayadas TN, Wagner DD. Vicinal cysteines in the prosequence play a role in von Willebrand factor multimer assembly. *Proc Natl Acad Sci U S A*. 1992;89(8):3531-3535.

17. Wagner DD, Mayadas T, Marder VJ. Initial glycosylation and acidic pH in the Golgi apparatus are required for multimerization of von Willebrand factor. *J Cell Biol*. 1986;102(4):1320-1324.

18. Horowitz B, Javitt G, Ilani T, et al. Quiescin sulfhydryl oxidase 1 (QSOX1) glycosite mutation perturbs secretion but not Golgi localization. *Glycobiology*. 2018;28(8):580-591.

19. Turecek PL, Mitterer A, Matthiessen HP, et al. Development of a plasma- and albumin-free recombinant von Willebrand factor. *Hamostaseologie*. 2009;Suppl 1(29):S32-38.

20. Javitt G, Khmelnitsky L, Albert L, et al. Assembly Mechanism of Mucin and von Willebrand Factor Polymers. *Cell*. 2020. *In press.*

21. Sali A, Potterton L, Yuan F, van Vlijmen H, Karplus M. Evaluation of comparative protein modeling by MODELLER. *Proteins*. 1995;23:318-326.

22. Mi LZ, Lu C, Nishida N, Walz T, Springer TA. Simultaneous visualization of the extracellular and cytoplasmic domains of the epidermal growth factor receptor. *Nat Struct Biol*. 2011;18(9):984-989.

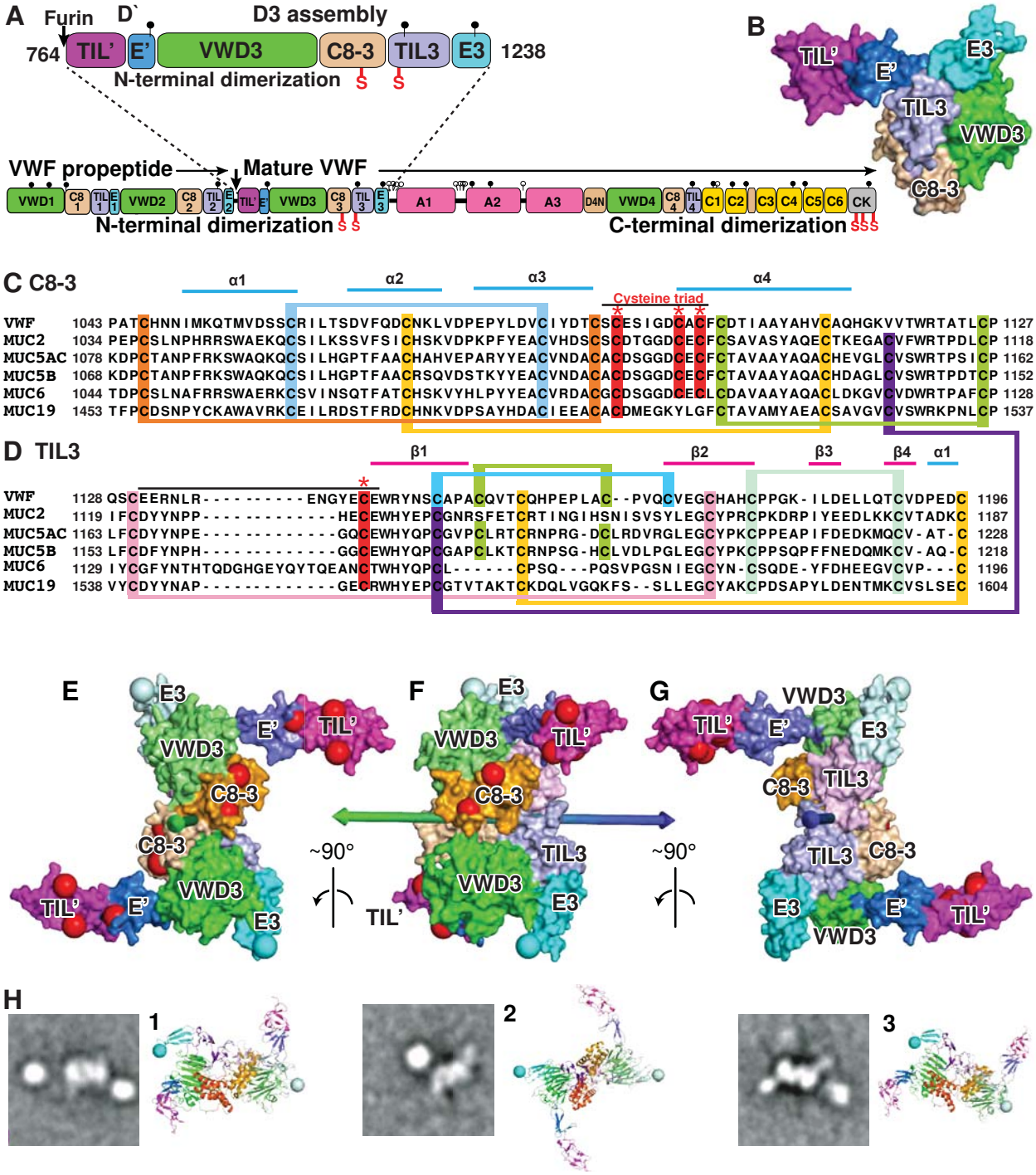

Figure 1

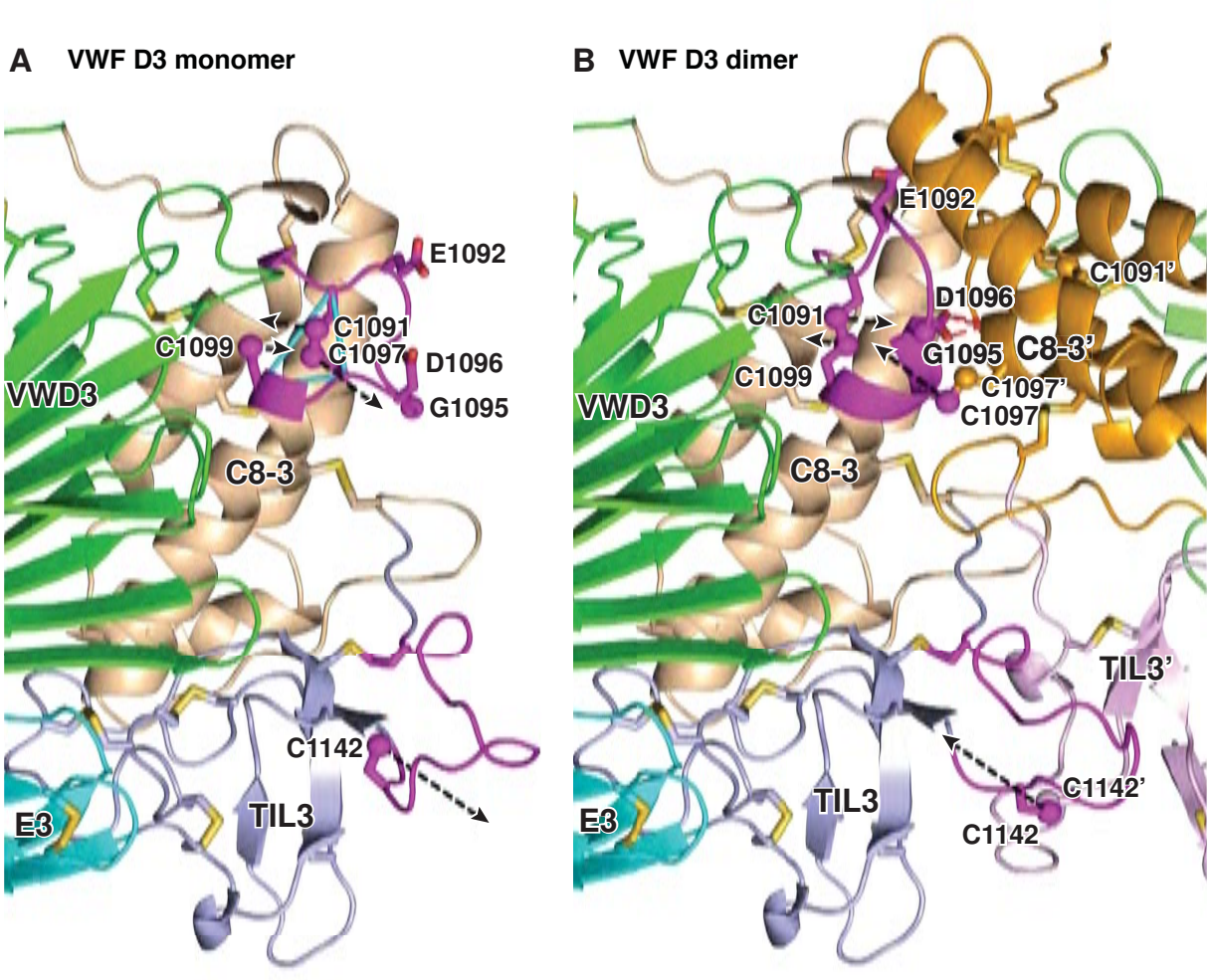

C

	1091			1095	1097	1099	
VWF mon.	S	C	E	S	I	G	D	C	A	C	F	α4-helix
VWF dim.	S	C	E	S	I	G	D	C	A	C	F	
MUC2 dim.	S	C	D	T	G	G	D	C	E	C	F	
MUC5AC	S	C	D	S	G	G	D	C	E	C	F	
MUC5B	A	C	D	S	G	G	D	C	E	C	F	
MUC6	G	C	D	S	G	G	D	C	E	C	L	
MUC19	A	C	D	M	E	G	K	Y	L	G	F	

Figure 2

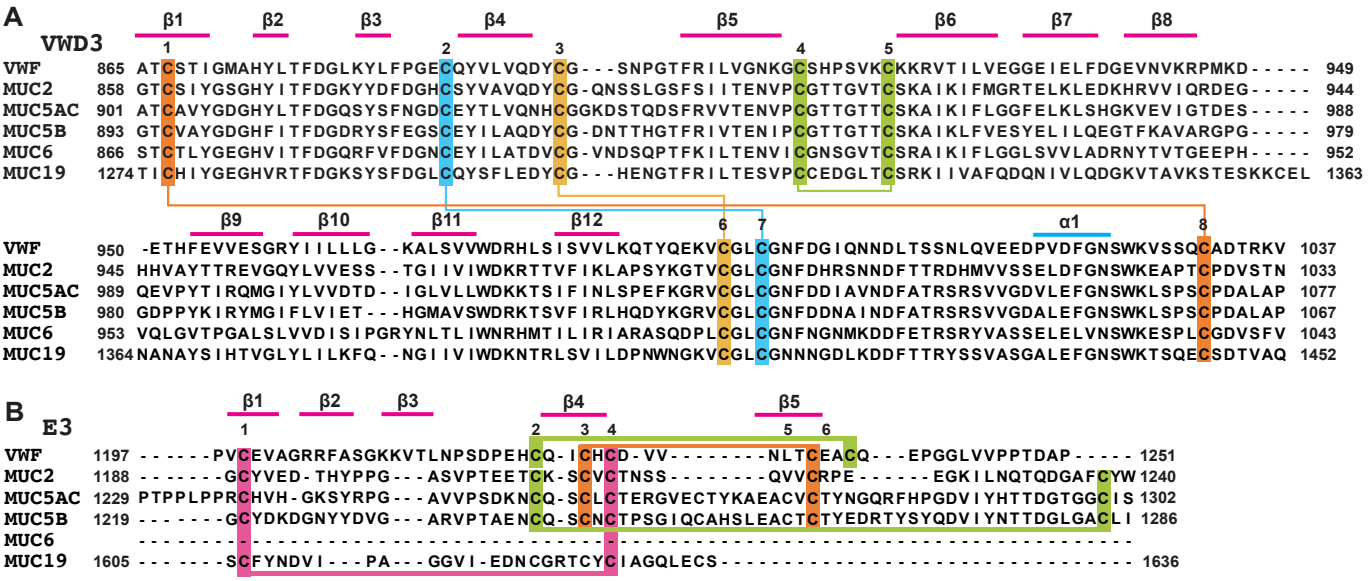

Supplemental Figure 1. Sequence alignments of D3 VWD3 and E3 modules in VWF and gel-forming mucins (see Main text Figure 1 for D3 C8-3 and TIL3 modules).

```
VWF Dimer  SLSCRPPMVKLVCPADNLRAEGLECTKTCQNYDLECMSMGCASGCLCPPGMVRHENRCVALERCPCFH
VWF  6N29  SLSCRPPMVKLVCPADNLRAEGLECTKTCQNYDLECMSMGCASGCLCPPGMVRHENRCVALERCPCFH
MUC2 6RBF  ------------------------------------------------------------------

VWF Dimer  QGKEYAPGETVKIGCNTCVCRDRKWNCTDHVCDATCSTIGMAHYLTFDGLKYLFPGECQYVLVQDYCG
VWF  6N29  QGKEYAPGETVKIGCNTCVCRDRKWNCTDHVCDATCSTIGMAHYLTFDGLKYLFPGECQYVLVQDYCG
MUC2 6RBF  ------------------------------------------------------------------

VWF Dimer  SNPGTFRILVGNKGCSHPSVKCAKRVTILVEGGEIELFDGEVNVKRPMKDETHFEVVESGRYIILLLG
VWF  6N29  SNPGTFRILVGNKGCSHPSVKCAKRVTILVEGGEIELFDGEVNVKRPMKDETHFEVVESGRYIILLLG
MUC2 6RBF  ------------------------------------------------------------------


VWF Dimer  KALSVVWDRHLSISVVLKQTYQEKVCGLCGNFDGIQNNDLTSSNLQVEEDPVDFGNSWKVSSQCADTR
VWF  6N29  KALSVVWDRHLSISVVLKQTYQEKVCGLCGNFDGIQNNDLTSSNLQVEEDPVDFGNSWKVSSQCADTR
MUC2 6RBF  ------------------------------------------------------------------

VWF Dimer  KVPLDSSPATCHNNIMKQTMVDSSCRILTSDVFQDCNKLVDPEPFYEACVHDSCSCDTGGDCECFCDT
VWF  6N29  KVPLDSSPATCHNNIMKQTMVDSSCRILTSDVFQDCNKLVDPEPFYEACVHDSC----------FCDT
MUC2 6RBF  ----------------------------------------------------CSCESIGDCECF---

VWF Dimer  IAAYAHVCAQHGKVVTWRTATLCPQSCEERNLRENGYECEWRYNSCAPACQVTCQHPEPLACPVQCVE
VWF  6N29  IAAYAHVCAQHGKVVTWRTATLCP----------------WRYNSCAPACQVTCQHPEPLACPVQCVE
MUC2 6RBF  ----------------------PIFCDYYNPP---HECEW--------------------------

VWF Dimer  GCHAHCPPGKILDELLQTCVDPEDCPVCEVAGRRFASGKKVTLNPSDPEHCQICHCDVVNLTCEACQE
VWF  6N29  GCHAHCPPGKILDELLQTCVDPEDCPVCEVAGRRFASGKKVTLNPSDPEHCQICHCDVVNLTCEACQE
MUC2 6RBF  ------------------------------------------------------------------
```

Figure S1